SEMARAK ILMU PUBLISHING

CFD Letters

Journal homepage:
https://semarakilmu.com.my/journals/index.php/CFD_Letters/index
ISSN: 2180-1363

The Comparison of Medical Grade PP with Common Grade PP in Injection Moulding Process

Muhammad Zulhilmi Mohd Zaki[1], Mohd Syakirin Rusdi[1,*], Calvin Ling Teck Xiao[1], Nur Sarah Zainal Abidin[1], Muhammad Amirul Farhan Mohd Shafee[1], Vimalraj A/L Tharumaalingam[1]

[1] School of Mechanical Engineering, Universiti Sains Malaysia, Engineering Campus, 14300, Nibong Tebal, Penang, Malaysia

ARTICLE INFO

Article history:
Received 10 December 2021
Received in revised form 23 March 2022
Accepted 24 March 2022
Available online 30 April 2022

Keywords:
Injection moulding; polypropylene; Medical grade PP; Common grade PP

ABSTRACT

Polypropylene (PP) is used to make a syringe and its tray, and there are two varieties of PP: medical grade (LB6331) and common grade (TP340). Although these two materials are basically similar, their characteristics differ significantly and have an impact on overall performance when made using the injection moulding process. The traditional trial-and-error method for optimising PP syringe and tray manufacture is often costly and time-consuming. This research is being done to create a numerical study using ANSYS Fluent on finding the best material to mass-produce the syringe and its tray to come up with a solution to lower the cost and time it takes to make the much-needed virus-fighting equipment. The objectives of this study are to compare the two types of PP's viscosity during injection moulding with ANSYS Fluent, to determine any incomplete fillings of both types of PP viscosity during injection moulding in the mould with ANSYS Fluent, and to compare the time taken between the two types of PP to fill up the mould casing. In the simulation, the temperature for both materials are set as 190 °C, and the parameter inserted beforehand are followed using the cross-parameter table, which contains zero shear viscosity, power-law index, and time constant for the temperature. A constant gauge pressure of 38.22 MPa is inserted as the inlet boundary condition for the simulation, along with the temperature of 190 °C. The results revealed that the time taken for the molten LB6331 to be fully injected into the mould is 1.5 seconds while for molten TP340 is 4 seconds. The viscosity of LB6331 at 2500 s^{-1} is approximately 220 Pa.s while the viscosity of TP340 is approximately 350 Pa.s. Both PP are shear thinning because their viscosity decreases with increasing shear rate. The VOF for both simulation of LB6331 and TP340 showed that there are imperfections at the edge of the mould casing because that part still contains air.

1. Introduction

Since vaccines to combat the Covid-19 is being distributed worldwide, demands for medical equipment such as syringes and its tray skyrocketed. The go-to manufacturing process to produce the mentioned medical equipment is the injection moulding process. While injection moulding is

* *Corresponding author.*
E-mail address: syakirin@usm.my (Mohd Syakirin Bin Rusdi)

https://doi.org/10.37934/cfdl.14.4.113

convenient when producing complex shapes such as a syringe, the materials used are critical when producing the equipment.

According to research from Maddah [1] and Ishak *et al.,* [2], a syringe and its tray are made up of polypropylene (PP), and there are two types of PP: medical grade and commercial grade. While these two are fundamentally similar materials, their properties differ slightly and affect the overall performance when manufactured with the injection moulding process. The conventional trial-and-error method commonly used to optimise the PP syringe and tray production are often expensive and slow.

Ramesh *et al.,* [3] demonstrated the simulation of injection moulding development and the optimization of vehicle instrument characteristics using various optimization approaches. The shrinkage volume rate and warpage quantity rate are measured using Taguchi Orthogonal parameter design and particle swarm optimization (PSO) in this paper. Most of the studies are aimed at calculating the decrease and warpage for different gate locations and glass types. The Taguchi orthogonal design has five parameters that are all inversely proportional to one another. As a result, the injection moulding method is passed out by optimising those settings. The purpose of this study is to use optimization strategies to process injection moulding for vehicle instrument parameters.

With the use of a visualisation mould, Wang *et al.,* [4] conducted a series of systematic tests to investigate the effects of different processing factors of high pressure foam injection moulding on packing efficiency such as gas concentration, packing pressure, packing time, injection speed, and melt temperature. This is to determine the time required for the gate-nucleated cells to fully dissolve. A drop in gas concentration or an increase in packing pressure considerably expedited the dissolution process, according to the results. The impact of injection speed and temperature on cell dissolution suggested that competing mechanisms were presence.

A research has been conducted by Nasiri and Khosravani [5] to study the implementation of an intelligent system to detect various defects in injection moulding. The study used fuzzy case-based reasoning (fuzzy CBR) method it can solves current problems based on nearest solutions of similar cases. The evaluation of the implemented system is done by detecting different faults in the manufacturing line. The acquired results showed the proposed system's capabilities and accuracy in fault identification.

Jachowicz *et al.,* [6] described how to analyse the suitability of a material for injection moulding using the results of a computer simulation of the injection process. Computer simulation of the basic phenomena that occur during the injection moulding filling, packing, and cooling phases yields a variety of results, including typical information on the suggested technological parameters of the process and the dimensional accuracy of the moulded part, as well as data on the processing machine's production efficiency and energy demand. Based on this data, it is possible to analyse the suitability of the polymer materials used in the simulation to create products from a certain industry, taking into consideration a variety of factors, most of which are of an economic or qualitative nature.

The numerical analysis of heat transmission in the car's radiation system was explored in this study from Hassan *et al.,* [7] by utilising pure water and water containing nano-fluid. The simulation method was carried out using ANSYS fluent version 16.1 using the Computational Fluid Dynamic (FCD) technique. When using the same boundary condition, the study was validated with experimental data, and the error was 8% based on simulation results. In addition, the flow rate was validated using the Nusselt number in both concertation 0.7 percent and 1 percent. The Nusselt number has been enhanced by increasing nano particle concertation, according to numerical analysis. The heat exchanger is activated when the number of Nusselt increases. The heat transmission of nanofluids was found to be strongly reliant on the concentration of nano particles, the flow parameters, and the weak temperature-dependent heat transfer conditions in earlier experiments.

George and Qureshi [8] stated that non-Newtonian fluid is a fluid that does not obey Newton's law of viscosity. The difference between non-Newtonian fluid and Newtonian fluid is that their viscosity is dependent on shear rate. In a Newtonian fluid, the relation between shear stress and shear rate is linear, and the coefficient of viscosity can be determined. In a non-Newtonian fluid, however, the relation between the shear stress and shear rate is different. Therefore, it will exhibit a time-dependent viscosity, which means the coefficient of viscosity cannot be determined.

Research from Chhabra and Richardson [9] showed that for non-Newtonian fluid they can change their viscosity under stress. If a force is applied to the fluid, the sudden application of stress can cause them to get thicker and act like a solid, or in some cases, it results in the opposite behaviour, getting "runnier" than before. When the stress is removed, the fluid will return to its earlier state.

Not all non-Newtonian fluid behave the same way when stress is applied. Some non-Newtonian fluids react because of the amount of stress applied, while others react due to the length of time that stress is applied. There are four types of non-Newtonian fluid which are thixotropic, rheopectic, shear thinning and shear thickening.

Coussot [10] stated that for the thixotropic, the viscosity of the fluid decreases with stress over time. This means the longer the time for the stress applied to the fluid, the runnier the fluid will be. Rheopectic fluid is the opposite of thixotropic fluid, where the fluid's viscosity increases with stress over time. The longer the time for the stress applied to the fluid, the thicker the fluid will be. Honey is thixotropic, while cream is rheopectic.

For shear-thinning, the viscosity decreases with increasing stress [11]. This means the higher the stress applied to the fluid, the runnier the fluid will be. Lastly, for shear thickening, the viscosity increases with increasing stress. The higher the stress applied to the fluid, the thicker the fluid will be. An example of shear thinning, and shear thickening fluid is tomato sauce and oobleck, respectively.

Optimization of the injection moulding is important to increase the productivity of the equipment. Therefore, this research is done to find the optimised materials of the injection moulding so that the filling time of the PP can be reduced to produce the syringe and its tray. Two types of PP are used in this research which are medical PP (LB6331) and common grade PP (TP340).

This study will involve molten polypropylene (PP), which is a shear-thinning non-Newtonian fluid. The shear rate and shear stress of molten PP are difficult to determine; however, the absolute relation between them since the shear stress can be obtained using the correction factor n in an experiment. The shear rate as a function of the shear stress from experimental data can be then obtained.

There are three objectives of this study. Firstly, to compare the viscosity of medical PP (LB6331) and common grade PP (TP340) during injection moulding with ANSYS Fluent. Next, the second objective is to compare the volume of fluid (VOF) of medical PP (LB6331) and common grade PP (T340) during injection moulding with ANSYS Fluent. The third objective is to compare the time taken between the medical PP (LB6331) and common grade PP (TP340) to fill up the mould case.

2. Theory

2.1 Volume of Fluid

The Volume of Fluid Method (VOF) is a free surface approximation numerical method. It is generally known as the Euler method. A grid, which can be stationary or non-stationary, is used to characterise Euler methods. In a non-stationary grid, the grid motion is determined by the change in surface shape [12]. This method helps to monitor the position and orientation of the surface. The flux motion is characterized by Navier-Stokes equations, which must be solved separately.

The approach is based on using a fractional function C, which is determined as an integral of the fluid functions in a cell's characteristics. C is a continuous function, with 0 ≤ C ≤ 1. If the cell is empty (i.e., there is no fluid), C = 0. If the cell is full, C = 1. Derivative of the fractional function must be equal to zero [13].

$$\frac{\partial c}{\partial t} + v \cdot \nabla C + \nabla \cdot [C(1-C)U_r] = 0 \quad (1)$$

where v denotes fluid velocity, and U_r denotes an artificial force that "compresses" the region under consideration.

The model's theory is based on the idea that another fluid cannot fill a fluid's volume at the same instant of time. As a result, each material is represented by a fraction, *f*, in a discrete volume cell. For any time and space, the number of the fractions of the fluids in a cell must equal 1. Since the fluids are moving, the fluid interface changes, requiring the fluid fractions to be changed.

The fractions of fluid in a cell can be classified into three types: if the cell is filled with fluid i, fraction $f_i = 1$; if the cell does not contain fluid i, fraction f_i = 0; and if the cell shares its volume with two or more fluids besides fluid i, the fraction of i takes a value $0 < f_i < 1$ [14].

The transport equation for pure convection is used to represent and update the interface of the material front:

$$\frac{\partial f}{\partial t} + \frac{\partial (u f_i)}{\partial x} + \frac{\partial (v f_i)}{\partial y} = 0 \quad (2)$$

where u is velocity component in x-direction while v is velocity component in y-direction.

Once the material front equation is solved, the interface between the participating fluids can be determined, implying the conservation of mass of one phase in the mixture. A multiphase problem is solved for the n − 1 phase, and the remaining phase is solved using equation below [14].

$$\sum_{i=1}^{n} f_i = 1 \quad (3)$$

where n is the fluid phase while f_i is the fluid fraction.

In this way, the fluid properties for the mixture of the two phases studied can be described from the following constitutive relations [14]:

$$\rho = (1-f)\rho_1 + f\rho_2 \quad (4)$$

$$\eta = (1-f)\eta_1 + f\eta_2 \quad (5)$$

where ρ is the fluid density while η is the apparent viscosity (Pa s).

2.2 Navier-Stokes Equation

The Navier-Stokes equations are the fundamental partial differential equations that explain the motion of viscous fluid substances. This equation is used to describe the flow of incompressible and frictionless fluid. This equation can be derived from continuity equations and conservation of energy [15]. The general form of continuity equation can be expressed as:

$$\frac{d\rho}{dt} + \nabla \cdot (\rho \vec{v}) + Q = 0 \quad (6)$$

where ρ is the fluid density, ∇ is divergence, $\vec{v}$ is the velocity component, and Q is heat transfer.

By applying the continuity equation to density, we will get the conservation of the mass equation [16]. We are also operating with a constant control volume. With no sources or sinks of mass (Q = 0), we obtain:

$$\frac{d\rho}{dt} + \nabla \cdot (\rho\vec{v}) = 0 \tag{7}$$

For incompressible fluids, density is constant. Therefore, the continuity equation can be expressed as [15]:

$$\nabla \cdot \vec{v} = 0 \tag{8}$$

Thus, the Navier-Stokes equation can be expressed as [15]:

$$\rho\left[\frac{\partial v}{\partial t} + (v \cdot \nabla)v\right] = -\nabla p + \rho\vec{g} + \mu\nabla^2\vec{v} \tag{9}$$

where ρ is the fluid density, v is velocity component, ∇ is divergence, μ is the fluid dynamic viscosity, and $\vec{g}$ is gravitational force.

However, the equation of Navier-Stokes can only be applied to Newtonian fluids. As for non-Newtonian fluids, power-law fluids can be used.

2.3 Power-law Fluids

Power-law fluids are different from Newtonian fluids in that the stress in a power-law fluid is raised to an exponent, n, called the flow behaviour index. For a Newtonian fluid [17]:

$$\tau = \mu\left(\frac{\partial u}{\partial y}\right) \tag{10}$$

where τ is shear stress, μ is dynamic viscosity, and $\frac{\partial u}{\partial y}$ is the shear rate.

Power-law fluids model the stress according to the equation [17]:

$$\tau = \mu\left(\frac{\partial u}{\partial y}\right)^n \tag{11}$$

where n is the power law index.

From Eq. (11), a Newtonian fluid is a power-law fluid with n = 1, making Newtonian fluids are a subset of power-law fluids [17]. For n < 1, the material can be specified as pseudoplastic, decreasing the viscosity as the shear stress increase. For n > 1, the material is specified to be dilatant, having increased viscosity when shear stress increases [18].

2.4 Cross WLF-Model

The effects of shear rate and temperature on viscosity are considered in this 6-parameter model. This model, like the Bird-Carreau model, accounts for both Newtonian and shear thinning [19]. The generic Cross equation is used to simulate the shear thinning component, which is a common and older alternative to the Bird-Carreau-Yasuda model [19]:

$$\frac{\eta_\gamma - \eta_\infty}{\eta_0 - \eta_\infty} = \frac{1}{1+(K\cdot\dot{\gamma})^{1-n}} \quad (12)$$

where η_0 is the zero-shear rate viscosity, η_∞ is an infinite shear rate viscosity, K is a time constant and n is the Power Law index, which indicates for the shear thinning behaviour. The well-known form of the Cross model can be expressed as Eq. (13) if the infinite shear rate viscosity is insignificant [19].

$$\eta(\dot{\gamma}) = \frac{\eta_0}{1+\left(\frac{\eta_0\dot{\gamma}}{\tau^*}\right)^{1-n}} \quad (13)$$

From Eq. (13), τ^* represents the critical shear stress at the transition from the Newtonian plateau, given $K = \frac{\eta_0}{\tau^*}$, and n is the Power Law index. Since it provides the best fit to most viscosity data, the Cross-WLF model is the most used model in injection moulding simulation software.

3. Methodology

3.1 Materials

Common grade polypropylene (TP340) and medical-grade polypropylene (LB6331) using WinRheo II software.

3.2 Equipment/Softwares

GÖTTFERT Rheograph 25 Capillary Rheometer, ANSYS Fluent.

3.3 Procedures

3.3.1 Collecting data from the capillary rheometer

A capillary rheometer controlled by a computer using LabRheo software is used to set the rheometer's measuring mode, steps, and temperature [20]. The capillary rheometer is manufactured by GÖTTFERT, as shown in Figure 1. The step option is used to adjust piston speed to control the shear rate of the non-Newtonian molten polypropylene. The temperature of the rheometer is set at 190 °C, 30 °C more than the melting temperature of the polypropylene. The parameters required to run the rheometer are set on the computer, then relayed to the rheometer machine. The pressure transducer is calibrated where the pressures P_1 and P_2 is set to zero. A piston is used to compress the polypropylene pellets until they are compact. The piston is then attached to its holder which the machine will further compress the pellets until 100 MPa. The pellets are added again until the neck of the capillary hole, compressed manually. A piston is used to compress the polypropylene pellets until they are compact. The piston is then attached to its holder which the machine will further compress the pellets until 100 MPa. The pellets are added again until the neck of the capillary hole, compressed manually. The capillary rheometer is cleaned by removing the two-pressure transducer and cleaning the capillaries. The data is collected from the computer, which is used for analysis. The experiment is repeated with the other type of polypropylene, whichever comes first at discretion.

Fig. 1. GÖTTFERT Rheograph 25 Capillary Rheometer

3.3.2 Comparing the injection moulding process between two grades of polypropylene using ANSYS fluent

Figure 2 show the real tray and the CAD model of the tray mould made using SolidWorks later converted into .iges file used in ANSYS fluent. This CAD model will be the base model for both molten polypropylenes (PP) simulated in ANSYS Fluent. ANSYS Workbench meshing is used to mesh the model and name their boundary conditions accordingly [21]. The parameters of common grade polypropylene (TP340) are inserted first (density, specific heat capacity, etc.) into ANSYS Fluent.

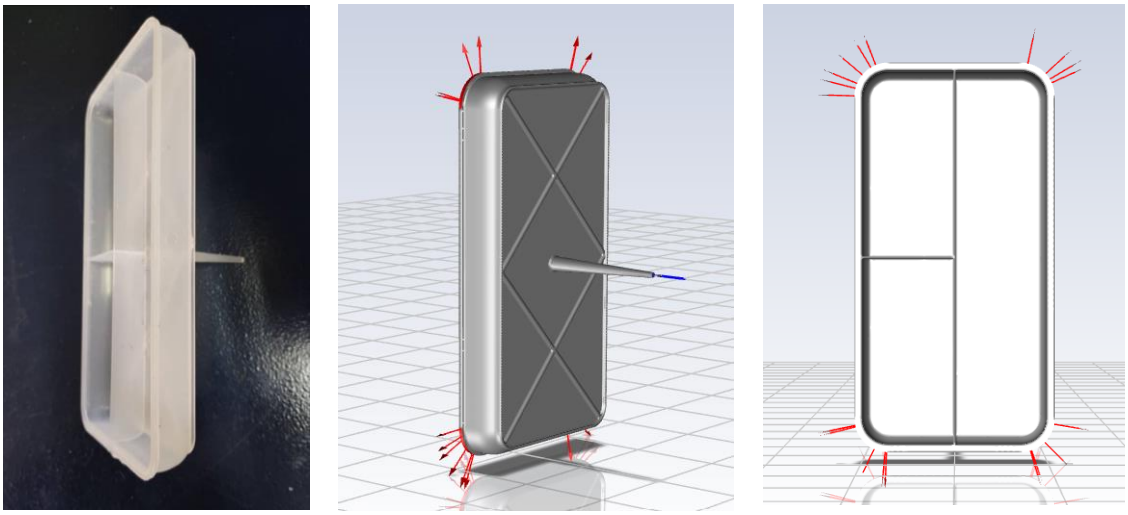

(a) (b) (c)

Fig. 2. (a) real tray, (b) side view, and (c) front view of the CAD model of the tray mould

Table 1 shows the simulation parameters for medical grade PP (LB6331) and common grade PP (TP340). The inlet temperature, inlet pressure, and density for both materials are constant which are 190 °C, 38.22 MPa, and 900 kg/m^3, respectively. The viscosity for both materials are followed using the cross-parameter table, which contains zero shear viscosity, power-law index, and time constant

for 190 °C. The outlet boundary condition is set with the outer temperature being 27 °C and is set as a 'static wall'. A simulation of 20 s is set using 400 000 timesteps, each timestep lasting 50 μs and the simulation file is autosaved for every 10 000 timesteps, which will be used to plot the graph the shear viscosity against time. The experiment is then repeated using the parameters of medical grade polypropylene (LB6331).

Table 1
Simulation parameters for both materials

Material	Medical grade (LB6331)	Common grade (TP340)
Inlet temperature (°C)	190.00	190.00
Inlet pressure (MPa)	38.22	38.22
Density (kg/m^3)	900	900
Zero shear viscosity (kg/m s)	2160.00	7830.00
Power law index	0.2590	0.3120
Time constant (s)	0.0573	0.3630

4. Results and Discussions

4.1 Time Taken for Both Molten PPs to Fill Up the Mould Casing Fully

The simulation aims to determine the time taken for the molten PP to fill the casing up at a volume of approximately fully 8.5 × 10^{-5} m^3 (Exact value: V = 8.565086 × 10^{-5} m^3. The value is taken from volume statistics in ANSYS 2021 Student Edition). The volume of the molten PP filling in the void at each autosaved timesteps is obtained using the following steps. Firstly, the 'Results' column is clicked, and the 'Volume Integrals button is accessed from the 'Reports' column. Next, the report type is set to 'Volume Integral', the field variable is set to 'Phases', with 'Volume fraction', and the 'pp190' (Molten PP at 190 °C) is set, and the cell zone is set to 'fluid'. Then, the total volume integral is computed, the output is recorded, and a graph of volume against time is plotted.

The graphs of molten common grad polypropylene (TP340) and medical grade polypropylene (LB6331) volume against time throughout the entire 400000 timesteps are shown in Figure 3 and Figure 4. The time taken for molten common grade PP (TP340) and medical grade PP (LB6331O to fill up the mould casing fully are determined. From Figure 3, it can be observed that the time taken for molten TP340 to be fully injected into the mould casing is approximately 4 seconds. The mould is filled when the volume reached 8.565086 × 10−5 m3.

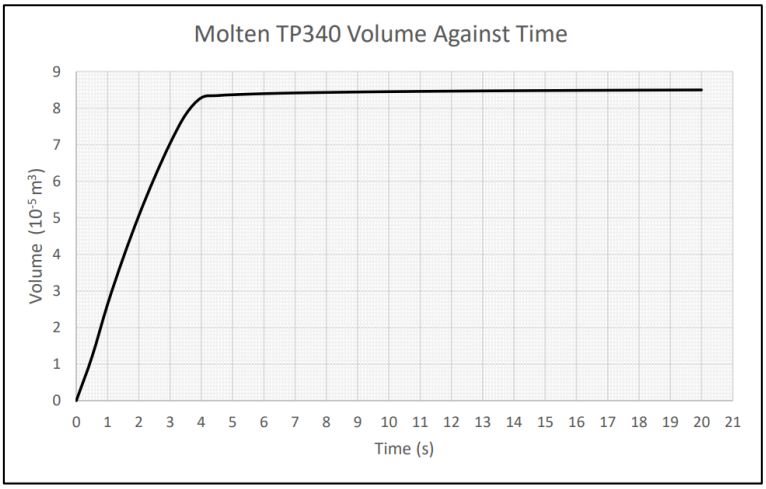

Fig. 3. Graph of Molten TP340 Volume against Time

For the molten LB6331, it can be observed that the time taken for molten LB6331 to fully fill the mould is approximately 1.5 seconds as shown in Figure 4 below. The time taken for the molten LB6331 to be fully injected into the mould is lower than the molten TP340. This is because the molten LB6331 has lower viscosity than molten TP340. The molten LB6331 resists motion less than molten TP340 because its molecular makeup gives it lesser of internal friction. When the viscosity of a fluid is higher, the more internal friction that it builds, causing to more time taken to be injected into the mould.

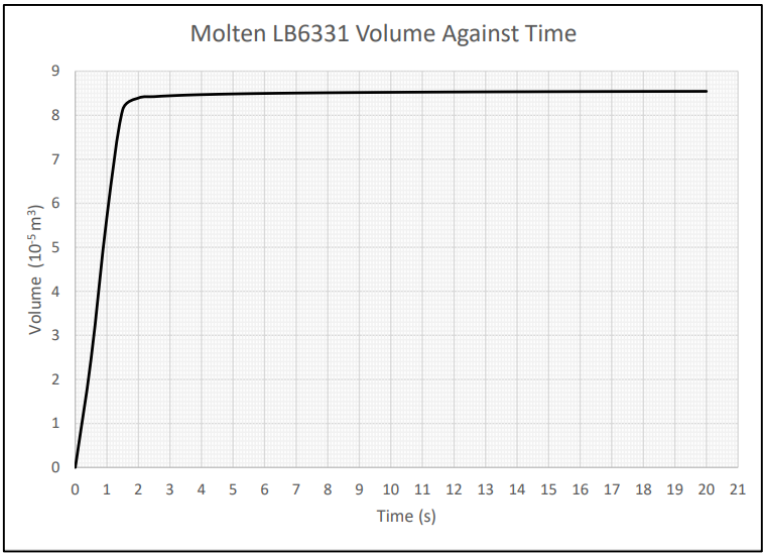

Fig. 4. Graph of Molten LB6331 Volume against Time

The simulation of both molten PP filling time is done using ANSYS Fluent. Total filling time is set as 20 seconds to see if the molten PP can fill the cavity. A simulation of 20 s is set using 400 000 timesteps, each timestep lasting 50 µs and the simulation file is autosaved for every 10 000 timesteps. Figure 5 shows the filling time for medical grade PP and common grade PP at 1 second of the injection simulation. It can be observed that for medical PP, it fills the cavity faster than the common grade PP. This is because the medical PP has lower viscosity than the common grade PP, made the medical PP easier to flow into the mould casing tray.

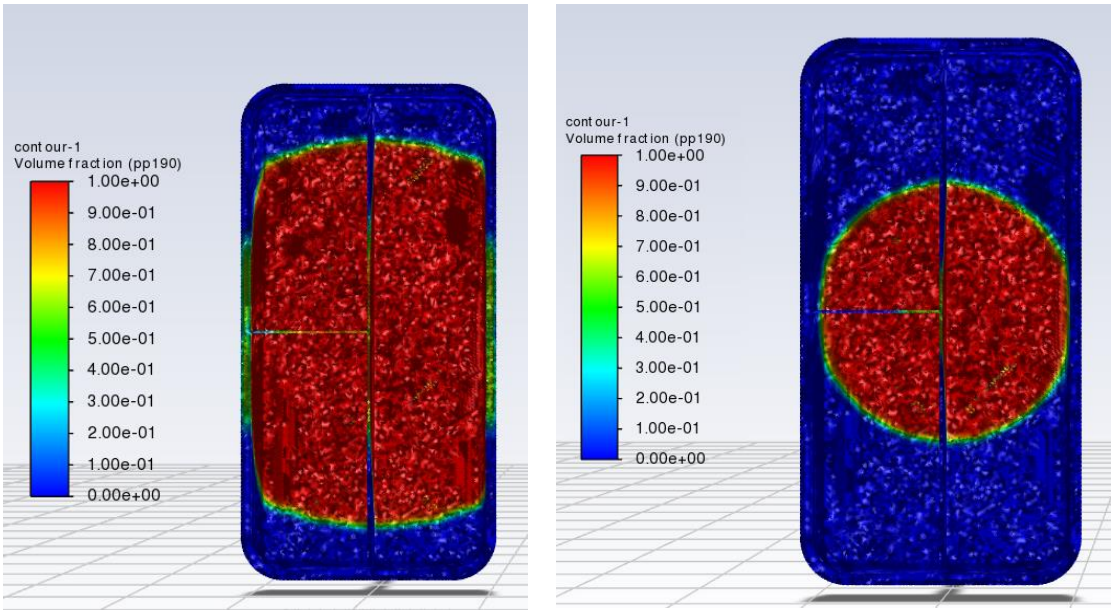

(a) (b)

Fig. 5. The molten PP of (a) medical grade PP (LB6331) and (b) common grade PP (TP430) filling the tray cavity at time = 1 second

4.2 The Viscosity of Both Molten PP Against its Shear Rate

It can be observed that when the strain rate increases, the viscosity of the polypropylene decreases exponentially. The changes in viscosity for LB6331 and TP340 indicate that the liquids are shear thinning because their viscosity decreases with increasing shear rate. Generally, the higher the rate of the decrease of viscosity as the shear rate increases, the easier the molten PP to flow into the mould tray casing to fill in. Figure 6 and Figure 7 show the relationship between viscosity and shear rate for common grade PP (TP340) and medical grade PP (LB6331) respectively. By comparing the two graphs, it can be observed that the LB6331 has lower viscosity than TP340. The viscosity of LB6331 at 2500 s^{-1} is approximately 220 Pa.s while the viscosity of TP340 is approximately 350 Pa.s. In addition, the higher shear rate combined with lower viscosity for the molten LB6331 PP contributes more to the higher rate of the molten PP injected into the mould tray casing compared to the molten TP340 PP.

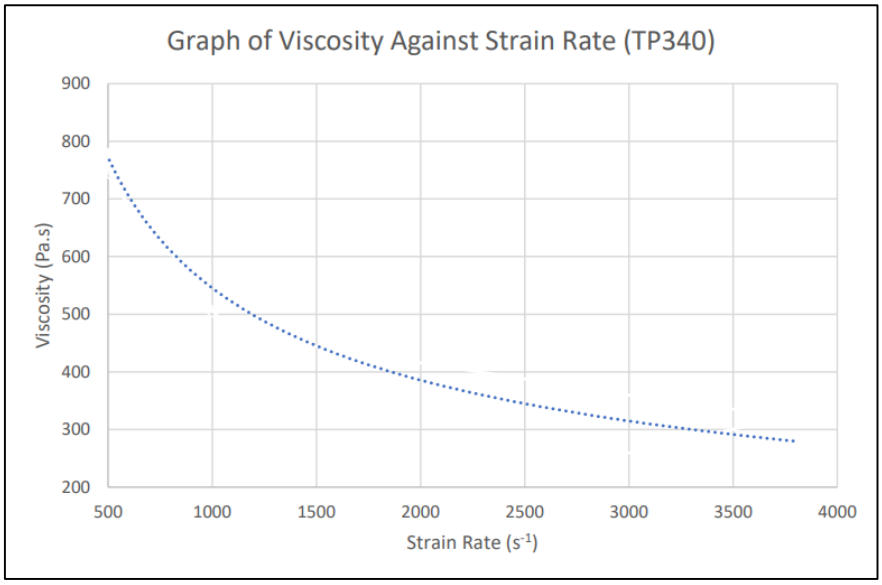

Fig. 6. Graph of Viscosity against Strain Rate (TP340)

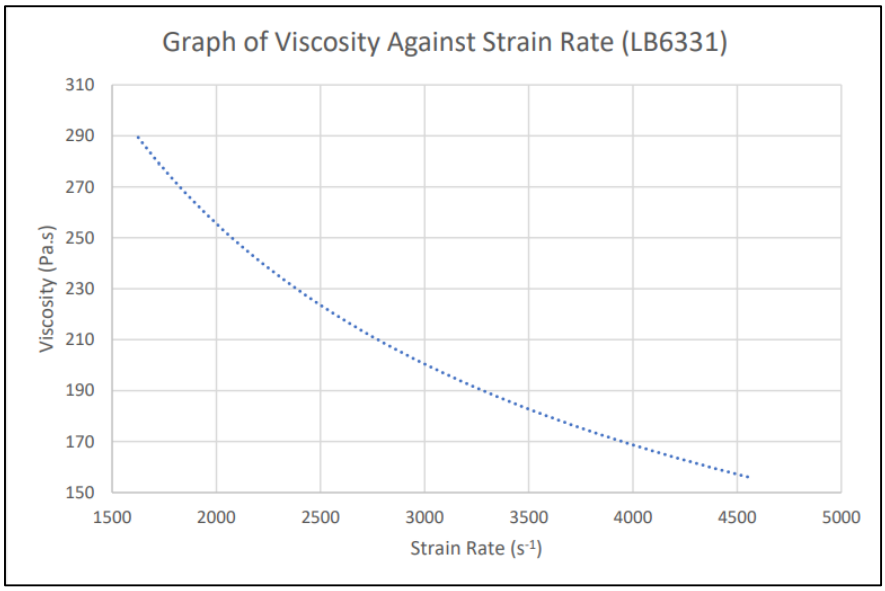

Fig. 7. Graph of Viscosity against Shear Rate (LB6331)

4.3 Imperfection Present in Both Molten PP using VOF

The Volume of Fluid (VOF) method is a numerical method present in ANSYS Fluent to determine or track a fluid's free surface in an interface, for instance, the mould casing. Both cases (TP340 and LB6331) have imperfections at the bottom corner at its front and back, respectively, as shown in Figure 8. It can be observed that there are imperfections at the edge of the casing mould because both molten PP did not fully fill that part. The blue colour at the edge of the mould indicates that there is still air in that part because the VOF value did not equal to one. When the VOF value equal to one, therefore the casing mould would be filled with PP with no excess air left. The molten PP did not reach that part for both types because of the edge part is small, making it difficult for the PP to squeeze in.

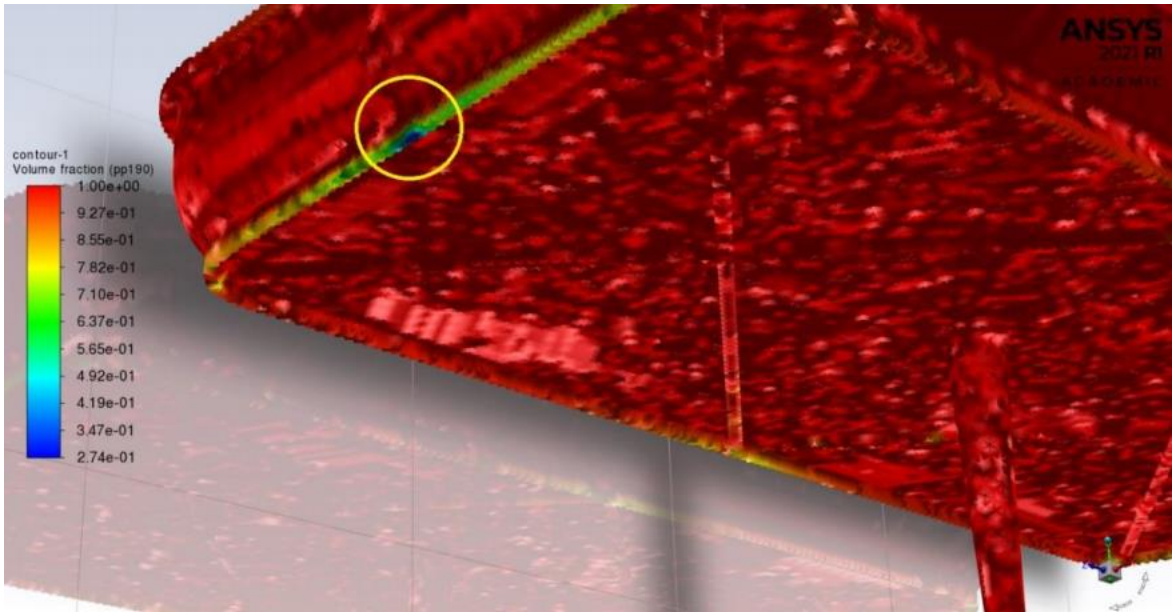

Fig. 8. Imperfections at the edge (yellow circle) (TP340)

5. Conclusions

In conclusion, the viscosity of the LB6331 is lower than TP340, making the time the LB6331 took to fill the mould is lesser than TP340. The time taken for LB6331 to fill the mould is approximately 1.5 seconds while TP340 is approximately 4 seconds. Both PP are shear thinning because their viscosity decreases with increasing shear rate. The viscosity of LB6331 at 2500 s^{-1} is approximately 220 Pa.s while the viscosity of TP340 is approximately 350 Pa.s. In addition, the higher shear rate combined with lower viscosity for the molten LB6331 PP contributes more to the higher rate of the molten PP injected into the mould tray casing compared to the molten TP340 PP.

The VOF for both simulation of LB6331 and TP340 showed that there are imperfections at the edge of the mould casing because that part still contains air. A better parameter, such as a higher temperature and pressure, will be required to further optimise the injection moulding process of these two materials so that the time it takes to produce each unit of the syringe and its tray is significantly reduced, lowering the overall production cost of medical equipment.

Acknowledgement

The authors acknowledge the support from the Short-Term Research Grant, Universiti Sains Malaysia (304/PMEKANIK/6315569).

References

[1] Maddah, Hisham A. "Polypropylene as a promising plastic: A review." *American Journal of Polymer Science* 6, no. 1 (2016): 1-11.

[2] Ishak, Mohd Nasri, Abd Rahim Abu Talib, and Mohammad Yazdi Harmin. "Material selection and design analysis of multi-purpose disposable safety syringe." *International Journal of Engineering & Technology* 7, no. 4 (2018): 214-220. https://doi.org/10.14419/ijet.v7i4.13.21358

[3] Ramesh, S., P. Nirmala, G. Ramkumar, Satyajeet Sahoo, G. Anitha, A. K. Gnanasekar, and J. Isaac JoshuaRamesh Lalvani. "Simulation process of injection molding and optimization for automobile instrument parameter in embedded system." *Advances in Materials Science and Engineering* 2021 (2021). https://doi.org/10.1155/2021/9720297

[4] Wang, Chongda, Vahid Shaayegan, Franco Costa, Sejin Han, and Chul B. Park. "The critical requirement for high-pressure foam injection molding with supercritical fluid." *Polymer* 238 (2022): 124388. https://doi.org/10.1016/j.polymer.2021.124388

[5] Nasiri, Sara, and Mohammad Reza Khosravani. "Faults and failures prediction in injection molding process." *The International Journal of Advanced Manufacturing Technology* 103, no. 5 (2019): 2469-2484. https://doi.org/10.1007/s00170-019-03699-x
[6] Jachowicz, Tomasz, Ivan Gajdoš, Vlastimil Cech, and Volodymyr Krasinskyi. "The use of numerical analysis of the injection process to select the material for the injection molding." *Open Engineering* 11, no. 1 (2021): 963-976. https://doi.org/10.1515/eng-2021-0094
[7] Hassan, Qais Hussein, Shaalan Ghanam Afluq, and Mohamed Abed Al Abas Siba. "Numerical Investigation of Heat Transfer in Car Radiation System Using Improved Coolant." *Journal of Advanced Research in Fluid Mechanics and Thermal Sciences* 83, no. 1 (2021): 61-69. https://doi.org/10.37934/arfmts.83.1.6169
[8] George, Herman F., and Farrukh Qureshi. "Newton's law of viscosity, Newtonian and non-Newtonian fluids." *Encyclopedia of Tribology* (2013): 2416-2420. https://doi.org/10.1007/978-0-387-92897-5_143
[9] Chhabra, R. P., and J. F. Richardson. "Non-Newtonian Fluid Behaviour." In *Non-Newtonian Flow and Applied Rheology*, pp. 1-55. Butterworth-Heinemann, 2008. https://doi.org/10.1016/B978-0-7506-8532-0.00001-9
[10] Coussot, P. "Introduction to the rheology of complex fluids." In *Understanding the Rheology of Concrete*, pp. 3-22. Woodhead Publishing, 2012. https://doi.org/10.1533/9780857095282.1.3
[11] Rosato, Dominick V., Donald V. Rosato, and Matthew V. Rosato. "INTRODUCTION." In *Plastic Product Material and Process Selection Handbook*, pp. 1-39. Elsevier, 2004. https://doi.org/10.1016/B978-185617431-2/50004-9
[12] Rezaeimoghaddam, Mohammad, Rasool Elahi, Mohammad Reza Modarres Razavi, and Mohammad B. Ayani. "Modeling of non-Newtonian fluid flow within simplex atomizers." In *Engineering Systems Design and Analysis*, vol. 49170, pp. 549-556. 2010. https://doi.org/10.1115/ESDA2010-25266
[13] Kunugi, T., K. Hara, T. Nagatake, and Z. Kawara. "Reconsideration of scaling measure for liquid-column break problem." In *AIP Conference Proceedings*, vol. 1547, no. 1, pp. 280-288. American Institute of Physics, 2013. https://doi.org/10.1063/1.4816877
[14] Moraga, Nelson O., Luis A. Lemus, Mario A. Saavedra, and Roberto A. Lemus-Mondaca. "VOF/FVM prediction and experimental validation for shear-thinning fluid column collapse." *Computers & Mathematics with Applications* 69, no. 2 (2015): 89-100. https://doi.org/10.1016/j.camwa.2014.11.018
[15] Brenner, Howard. "Navier-Stokes Revisited." *Physica A: Statistical Mechanics and Its Applications* 349, no. 1-2 (2005): 60-132. https://doi.org/10.1016/j.physa.2004.10.034
[16] Fanchi, John R. " Reservoir Simulation." In *Integrated Reservoir Asset Management*, pp. 223-241. Gulf Professional Publishing, 2010. https://doi.org/10.1016/B978-0-12-382088-4.00013-X
[17] Mount III, Eldridge M. "Coextrusion equipment for multilayer flat films and sheets." In *Multilayer Flexible Packaging*, pp. 99-122. William Andrew Publishing, 2016. https://doi.org/10.1016/B978-0-323-37100-1.00007-7
[18] Baird, Donald G. "Polymer Processing." In *Encyclopedia of Physical Science and Technology*, pp. 611-43. Academic Press, 2003. https://doi.org/10.1016/B0-12-227410-5/00593-7
[19] Mishra, Ases Akas, Affaf Momin, Matteo Strano, and Kedarnath Rane. "Implementation of viscosity and density models for improved numerical analysis of melt flow dynamics in the nozzle during extrusion-based additive manufacturing." *Progress in Additive Manufacturing* 7, no. 1 (2022): 41-54. https://doi.org/10.1007/s40964-021-00208-z
[20] Rusdi, M. S., M. Z. Abdullah, A. S. Mahmud, C. Y. Khor, Abdul Aziz, Z. M. Ariff, and M. K. Abdullah. "Numerical investigation on the effect of pressure and temperature on the melt filling during injection molding process." *Arabian Journal for Science and Engineering* 41, no. 5 (2016): 1907-1919. https://doi.org/10.1007/s13369-016-2039-0
[21] Rusdi, M. S., M. Z. Abdullah, MS Abdul Aziz, M. K. Abdullah, A. A. Bakar, M. H. S. Abd Samad, P. Rethinasamy, Sivakumar Veerasamy, and C. Y. Khor. "Numerical Investigation on the Effect of Squeegee Angle during Stencil Printing Process." In *Journal of Physics: Conference Series*, vol. 1082, no. 1, p. 012057. IOP Publishing, 2018. https://doi.org/10.1088/1742-6596/1082/1/012057